DTM Extraction of Lidar Returns Via Adaptive Processing

Hyun S. Lee, *Student Member, IEEE,* and Nicolas H. Younan, *Senior Member, IEEE*

***Abstract*—Airborne light detection and ranging is emerging as a tool to provide accurate digital terrain models (DTMs) of forest areas, since it can penetrate beneath the canopy. Although traditional techniques, such as linear prediction, have shown to be robust type methods for the extraction of DTMs, they fail to effectively model terrain with steep slopes and large variability. In this paper, a modified linear prediction technique, followed by adaptive processing and refinement, is developed. A comparison with the traditional linear prediction method is provided along with statistical measures to ascertain the validity of the foregoing technique.**

***Index Terms*—Adaptive processing, digital terrain model (DTM), Light Detection and Ranging (LIDAR), linear prediction.**

I. Introduction

DIGITAL terrain models (DTMs) have received great attention due to their wide applications in the fields of surveying, civil engineering, geology, mining engineering, landscape architecture, road design, flood control, agriculture, planning, military operation, and forest management [1]. The trees' heights are of particular interest due to their usefulness in forest management. The overall tree heights have shown direct effects on several factors including the quality of logs and the wood volume. There exist a relationship between the height and other tree characteristics such that the height can be a useful factor in estimating the stem diameter and the quality of timber product as well [2].

If field sampling is sufficiently intense, ground-based survey works can produce very accurate results. However, this method is labor intensive, and it is not always possible to secure the services of well-trained field workers; moreover, the financial resources are often limited. Traditionally, photogrammetry can be used for the construction of DTMs, and the accuracy of photogrammetrically derived DTMs in open areas is satisfactory. However, in dense forest areas, it is expected that photogrammetry-type techniques cannot extract the terrain information under dense trees.

Light Detection And Ranging (LIDAR) is a technique in which light is used to measure the range between a target and a sensor. It is an active remote sensing technology that has now become commercially widespread. Airborne scanning LIDAR (ASL) is a measurement system in which pulses of light are emitted from an instrument mounted in an aircraft. The travel time of a pulse of light from the sensor to the reflecting surface and back is used to determine the range to the surface. These types of systems typically record the range to the highest reflecting surface only within the laser footprint. If the laser beam is reflected from the top or the lower branches of a tree, a measured vegetation point will lie too high with respect to the terrain [3]. Airborne LIDAR systems can generate range measurements at rates of up to 30 000 times/s, with the laser beam scanning across the flight path as the aircraft moves across the terrain. The high pulse repetition rates of these types of LIDAR systems mean that in vegetated areas at least some of the measurements will correspond to the underlying ground surface. Thus, the generation of DTMs of the underlying ground surface is possible, even in dense forestry. The first step in this generation is to distinguish the laser scanner data into terrain and nonterrain points (in the wooded areas, these points are called vegetation points). In areas with infrequent canopy gaps, this can become difficult [3].

Several techniques have been used to derive DTMs with small-footprint LIDAR systems. Although small-foot print LIDAR data are not used directly, Blair *et al.* have shown that the vertical structure for vegetation contained in a large-footprint laser altimeter return waveform using a laser return data with small-footprint size can be estimated [4]. Their method has indicated that large-footprint laser altimeters can model the laser return waveforms as the sum of the elementary pulses reflected from each element in the footprint, since they can be used to represent the vertical distribution of intercepted surfaces within an individual footprint.

Kilian *et al.* introduced a windowing technique that interpolates ground models in forestry [5]. Intervals, known also as windows, can be selected to determine ground points within a specific interval. The lowest point in the window, as well as all other points within a certain height above the lowest point, was considered to be ground points. A weight was then assigned to each point depending on the window size and surface interpolation was carried out. However, for a good model interpolation, this process was repeated for several window sizes, and the resulting model was window-size dependent. This technique was later improved by using a linear prediction method to determine terrain models in wooded areas with airborne laser scanner data [6], [7]. Accordingly, a rough surface approximation was first determined. Then, a modified weighting function resulting from robust adjustment was used to compute the weights from the residuals. Last, each measurement was given a weight according to its residual, where points with high weights were considered to be at the surface, whereas points with low weights were considered to be vegetation points; thus, they were disregarded in the interpolation process. However, this method fails to model

Manuscript received November 16, 2001; revised December 30, 2002.

The authors are with the Department of Electrical and Computer Engineering, Mississippi State University, Mississippi State, MS 39762-9571 USA (e-mail: younan@ece.mstate.edu).

Digital Object Identifier 10.1109/TGRS.2003.813849

terrain with steep slopes and large variability, and the computational time is quite extensive. In addition, lower points can be easily misclassified as ground points as a result of the occurrence of negative errors, i.e., ranging errors that appear as elevation points below the surface due to measurements misdetection by the sensor.

Recently, a segmentation-based method was developed to extract DTMs from three-dimensional height models [8]. First, the cloud of (x, y) and z coordinates are transformed into a grid. Then, the segmentation step implemented as prefiltering, seed point extraction, and seeded region growing is processed. This technique is shown to be robust as well.

In this paper, a combined modified linear prediction and an adaptive processing technique is developed to extract ground elevation models collected by range-only small-footprint LIDAR systems in the presence of vegetation. This technique extends the existing work of Pfeifer and Kraus [3], [6], [7], where the ground points obtained from the linear prediction are compared with the original measurement points to extract matched points, i.e., points with the same (x, y) coordinates as the measurements but with different height z values, and then perform interpolation for refinement purposes. The adaptive filtering technique, on the other hand, can be thought of as a postprocessing step, which eliminates spurious peaks adaptively. Results obtained from this modified technique are presented, and a comparison with the traditional linear prediction method is provided along with statistical measures to ascertain the validity of the foregoing technique.

II. Linear Prediction

The linear prediction method is based mainly on calculating the residuals, i.e., the distance from the surface to the measurement points, for all z measurements (elevation points) as a starting point. Intuitively, it is assumed that terrain points are more likely to have negative residuals, whereas vegetation points are more likely to have positive residuals. These residuals are then used to compute weights, or prediction coefficients, for each measurement using a special weight function as depicted in Fig. 1 [3]. Note that the origin of the weight function is placed at a negative value g rather than the zero value, since the data points with negative residuals are kept.

One key step in choosing such a weight function is to select the optimum value g. Three ways to find the optimal value of g have been used. The first method uses the expected accuracy of the terrain points. This accuracy depends on the terrain slope. The origin of the histogram of the residuals is shifted to the left until the negative branch (residuals with negative values) reaches the expected standard deviation (chosen arbitrary). However, if there are large negative blunders, it is known that this method does not work well. The second method requires a rough estimation of the penetration rate. If it is estimated that 40% of the LIDAR points refer to ground points, the value of g is at the position where the first 20% of the residuals are found. For the third method, the standard deviation of the left branch is calculated and plotted for all possible shifts of the origin. The minima, from the plotted curve, are then searched and taken as possible values for g. In this paper, the third method

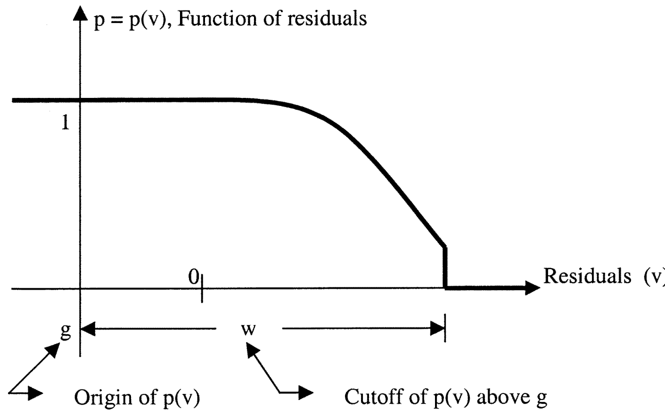

Fig. 1. Weighting function associated with the prediction coefficients.

is used, where the origin of the histogram is shifted to the left, until the negative branch reaches the standard deviation of the ground points σ_G[7]. This shift is the value for g. It can be defined as

$$\sigma_m^2 = \frac{\sum_{i=1}^{n_m} (v_i - m)^2}{n_m}, \qquad \text{for all } v_i < m. \tag{1}$$

Here v_i is the ith residual, and n_m is the number of residuals with $v_i < m$. Note that if $\sigma_m = \sigma_G = 0.8$, then, $g = m$.

Overall, these methods for finding the origin of the weight function g do not always produce good results [6]. This is further improved through the following interpolation scheme [7], [9]. Given a set of surface points $\{P_i\}$ with corresponding heights $\{z_i\}$, the main purpose is to achieve surface interpolation at any point P with a corresponding height z_P. The height z_P at any interpolated point can be obtained directly from

$$z_P = \mathbf{c^T C^{-1} z} \tag{2}$$

where $\mathbf{z}$ is a vector representing the heights of all available surface points $\{P_i\}$, i.e.,

$$\mathbf{z} = \{z_i\} = [z_1, z_2, \ldots, z_n]^T. \tag{3}$$

$\mathbf{C}$ is the covariance matrix whose elements represent the covariance between any two given available surface points, $C_{ik} = C(P_i P_k)$, which are derived from the Gaussian variogram model of kriging theory [10], i.e.,

$$C_{ik} = \begin{cases} \sigma_i^2 + C_0, & i = k \\ C_0 e^{-(d_{ik}/s)^2}, & i \neq k \end{cases} \quad i, k = 1, 2, \ldots, n \tag{4}$$

where d_{ik} refers to the horizontal distance between the ith and kth surface points P_i and P_k, i.e., $d_{ik} = P_i P_k$; C_0 is the covariance for a distance of zero, i.e., the value of C_{ik} when $d_{ik} = 0$; s is a parameter that controls the steepness of the covariance function, and it can be estimated directly from the available points; σ_i^2 is the measurement accuracy associated with $\{P_i\}$; and $\mathbf{c}$ is a vector representing the covariance between any arbitrary point P and a given available point $C(PP_k)$ on the surface, i.e.,

$$\mathbf{c} = [C(PP_1), C(PP_2), \ldots, C(PP_n)]^T. \tag{5}$$

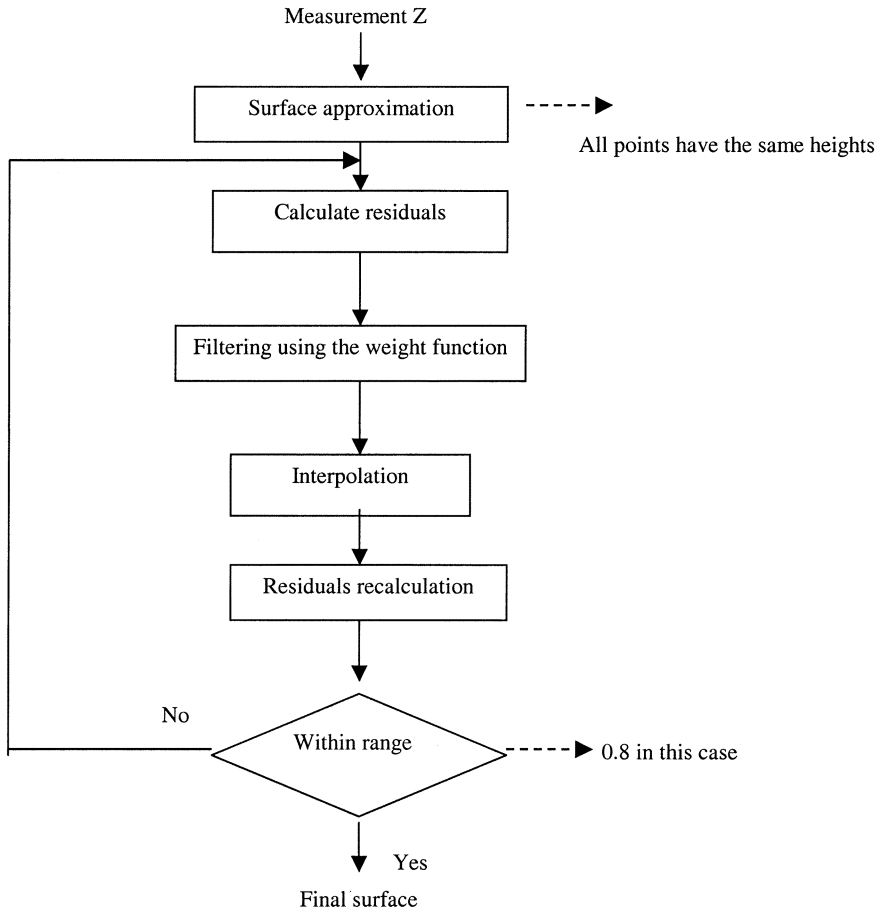

Fig. 2. Linear prediction implementation flowchart.

The basic steps for computing the surface are as follows. In the first step, the surface is computed with equal weights for all points. This estimated surface corresponds to the average points between terrain points and vegetation points. Next, the residuals are computed to find the appropriate weights for each measurement, and the weights can be used for the computation of the surface. Then, the residuals can be recomputed. If a residual is within a predefined specified range, the corresponding measurement z will be used again in the next iteration step. A flowchart of the linear prediction-based method for extracting DTMs is depicted in Fig. 2.

III. Modified Linear Prediction

The modified linear prediction presented in this investigation is an extension to the existing work presented by Pfeifer and Kraus [3], [6], [7], [9], where the ground points obtained from the linear prediction filtering are compared with the original measurement points to extract the matched points with the same (x, y) locations as the measurements and then perform interpolation for refinement purposes. Accordingly, the modified scheme used here is summarized as follows.

```
Step 1: Compute the mean of the measurements Z (the
mean is not constant in this case).
Step 2: Calculate the residuals.
Step 3: Set up the special weighting function using
the residuals
Step 4: Perform linear prediction filtering
Step 5: Compare the points obtained by Step 4 with
the original measurement points
Step 6: Extract the matched points, i.e., points
with the same (x, y) locations as the measurements
Step 7: Check the result. If satisfactory continue,
If not, go to Step 1
Step 8: Interpolation using (2)-(5).
```

In Step 1, since the measurements do not have a constant mean, a sample average for the whole data range is not appropriate. Assuming data ergodicity, the simplest method to estimate its mean is by using a sample average over a given window. However, if the window size is too small, large variability in the data mean is introduced. A window size of 800 is shown to be sufficient to avoid the variability in the mean [11]. From the mean values, the residuals for each measurement are then computed (Step 2). Note that Steps 2–4 are the same as in the ones used in the traditional linear prediction method. All steps performed after Step 4 are the extension steps, where Steps 5 and 6 are called “refinement” steps. The purpose of these steps is mainly to eliminate points generated in different positions with respect to the positions of the original measurement points, thus keeping all points with the same position. In Step 7, the penetrating rate, i.e., the ratio of the matched points of Step 6 to the total number of measurement points, is set to 30%. Therefore, the above steps are repeated until it satisfies the rate. A flowchart describing this process is illustrated in Fig. 3.

IV. Adaptive Prediction

An adaptive predictor scheme is used for constructing DTMs of ground surface from small-footprint LIDAR data. In the adaptive filter stage, the normalized least mean square (NLMS), one of the variants of the least mean square (LMS) algorithm, is applied. In general, the NLMS is used in applications where the input signal is subject to wide fluctuation, which is the case under investigation. The basic LMS algorithm can be summarized as follows [12]:

$$y(n) = \sum_{m=1}^{M} w_m(n)x(n-\Delta-m), \qquad n=0,1,\ldots,N\text{–}1 \quad (6)$$

$$e(n) = x(n) - y(n) \quad (7)$$

$$w_m(n+1) = w_m(n) + \mu e(n)x(n\text{–}\Delta\text{–}m), \qquad 1 \leq m \leq M \quad (8)$$

where $x(n)$ is the input signal representing the terrain points generated in Section III; $y(n)$ is the filter output; $w(m)$ are the filter coefficients of order M; $e(n)$ is the error signal; Δ is the delay factor or decorrelation parameter; and μ is the step size or adaptation parameter. This version of the LMS is known as adaptive line enhancement (ALE) [13]. Some of the main advantages of the ALE are its capability of automatically turning itself off when no SNR improvement is achieved and its on-line implementation for real-time processing. A block diagram of the ALE along with the "refinement" and interpolation stages is depicted in Fig. 4.

A direct implementation of the ALE algorithm requires *a priori* knowledge of the delay factor Δ, the adaptation parameter μ, and the filter order M. Careful considerations need to be taken when choosing the above parameters. The performance of the adaptive algorithm depends on appropriately selecting these parameters. It has been shown that the delay factor depends on the correlation between the true samples of the input signal $x(n)$ and the spurious interference present in $x(n)$. The adaptation parameter μ controls the speed of convergence (stability) of the filter coefficients $w(n)$. Consequently, μ must be properly selected to ensure convergence. In addition to appropriately choosing the decorrelation and adaptation parameters, selecting a filter order (filter length) plays a major role in the performance of the adaptive line enhancer. When the filter order M is sufficiently long enough (optimum value), the filter coefficients converge to their true values by reaching the steady-state solution.

Since, the stability, convergence, as well as the steady-state properties of the ALE depend on the filter length, the adaptation parameter, and the power of the input signal $x(n)$, it is appropriate to normalize the adaptation parameter by a factor of

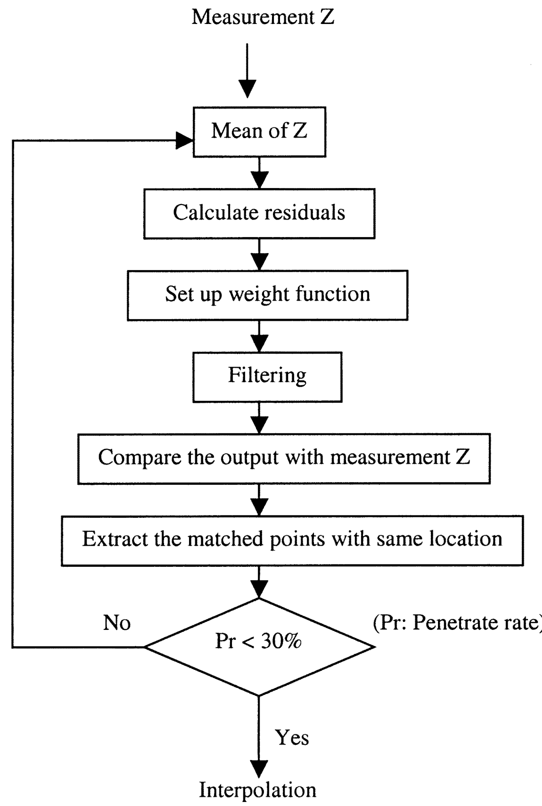

Fig. 3. Modified linear prediction implementation flowchart.

$\|x(n)\|^2$. This leads to the NLMS filter coefficients update. Accordingly [13]

$$w_{n+1} = w_n + \mu \frac{x(n)}{\|x(n)\|^2} e(n). \quad (9)$$

The aim of the adaptive filter is to perform a postprocessing to eliminate some spurious peaks caused by linear prediction. After the filtered output $y(n)$ is obtained, it goes through the "refinement" and "interpolation" steps to determine the corresponding DTM. As in the modified linear prediction, the "refinement" step is used for extracting match points with the same (x, y) locations as the measurement points. Fig. 5 illustrates the effect of the "refinement" stage by comparing the elevation points obtained from adaptive filtering with the original measurement points at the same y location. Note that only the elevation points extracted at the locations are kept and carried out to the next stage.

V. Results

In this study, LIDAR data, collected by EarthData, from a commercial forestland owned by the Trillium Corporation, near Bellingham, WA, were used. This site has variable terrain with a range of canopy densities and heights. The area of this site covers approximately 40 ha. The data were obtained in forested terrain. Each pulse shot may have one or multiple returns depending on the reflected surface. For instance, a first return is produced as a result of a reflection of an outgoing pulse from a top of a tree. The remainder of the pulse continues downward. Part of it may then be reflected from somewhere within

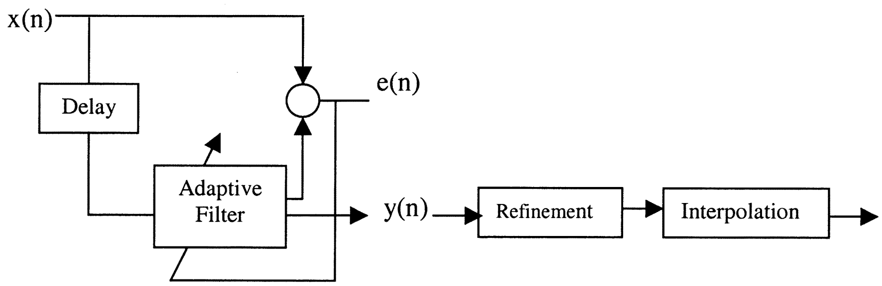

Fig. 4. Adaptive prediction scheme.

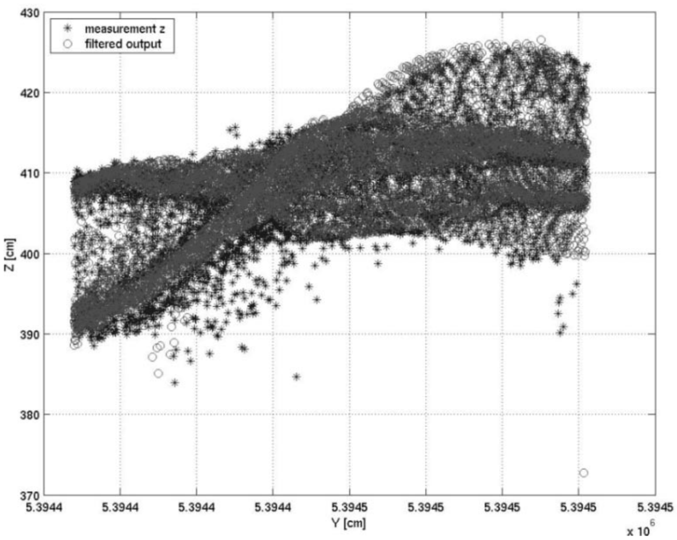

Fig. 5. "Refinement" stage effect.

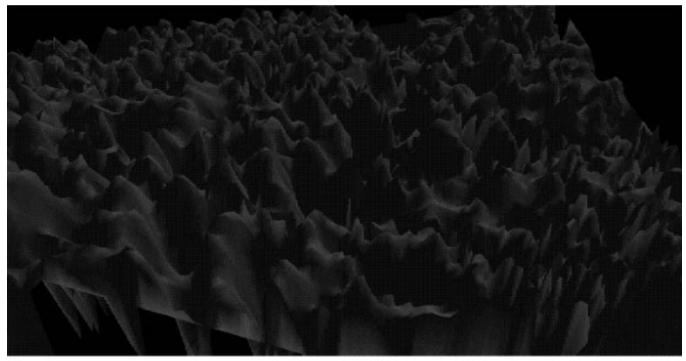

(a)

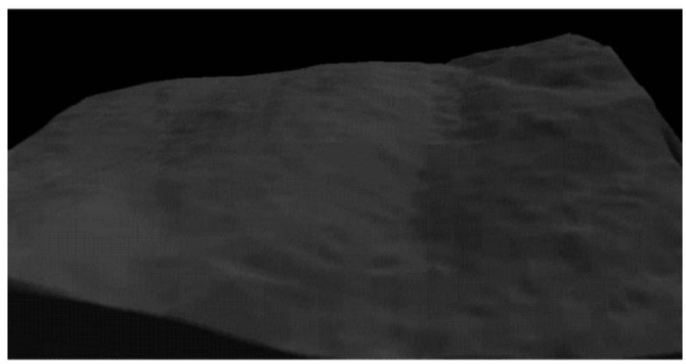

(b)

Fig. 6. LIDAR data images of the Bellingham site. (a) Image of the last return data. (b) Bare earth extracted from the last return data of (a) using automated and manual editing.

the canopy and produces a second return. In a similar manner, multiple returns can be detected. Shots are tagged to indicate that returns from 2, 3, or 4 reflecting surfaces are captured and the data associated with the last return are used, since they are likely to contain terrain points.

For the adaptive implementation, the step size and filter lengths are set to 0.9 and 50, respectively. Delay choices of 1, 10, and 20 are used for illustrative purposes. The resulting bare earth images are obtained using the ERDAS *Imagine Virtual GIS tool*. The images are georeferenced to the UTM projection system. The spheroid is GRS1980; zone number is 10; and datum is NAD83. Note that the viewing information of all images is field of view (FOV) is 50°; pitch is $-29°$; and azimuth angle is 2°. The pixel sizes of x and y are set to 0.2 m. Fig. 6(a) and (b) illustrates the images produced from the last return raw data as well as the bare earth model extracted from the last return using automated and manual editing. Note that EarthData has also provided the bare earth data. The collection of the bare earth data was achieved by passing a search window over the field area to inquire LIDAR raw points from all returns (first, second, etc.). Some points were regarded as points associated with the terrain surface and labeled as being "ground" points. Others were labeled as "features" above the ground. This process was repeated until all points in the field area were classified, and a good representation of the ground surface was obtained. Manual editing was then carried out to remove noise from patches of dense canopy [2].

The resulting bare earth images extracted from the last return of Fig. 6(a) using linear prediction, modified linear prediction, as well as adaptive filtering are illustrated in Fig. 7. It is clearly seen that the terrain image of Fig. 7(b) obtained from the modified linear prediction is smoother than the one obtained directly from the linear prediction of Fig. 7(a). Note that the traditional linear prediction generates spurious peaks caused by filtering, since all points inside a predefined threshold are considered to be ground points. This can be reduced by Steps 5 and 6 of the modified linear prediction. Spurious peaks can be further reduced by adaptive filtering as indicated in Fig. 7(c)–(e). Although all techniques extract bare earth models to a satisfactory level, the adaptive technique is shown to be better in terms of tracking the valleys and eliminating spurious peaks. For this experimental LIDAR data, the digital terrain image generated by the adaptive technique with a delay value 10 has the best

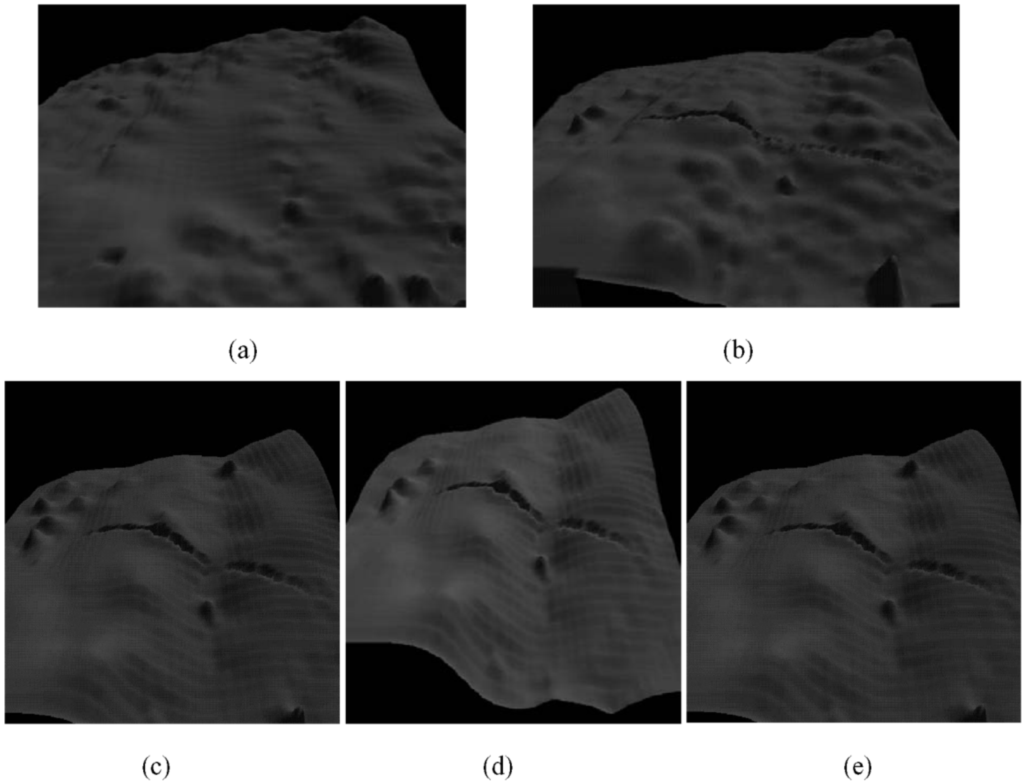

Fig. 7. Comparison of bare earth models extracted from the last return data of Fig. 6(a). (a) Linear prediction. (b) Modified linear prediction. (c) Adaptive processing (delay $= 1$). (d) Adaptive processing (delay $= 10$). (e) Adaptive processing (delay $= 20$).

TABLE I
QUANTITATIVE QUALITY COMPARISONS OF EXTRACTED BARE EARTH MODELS. UNITS ARE IN CENTIMETERS

	Adaptive Delay=1	Adaptive Delay=10	Adaptive Delay=20	Modified Linear Prediction	Linear Prediction
RMSE	6.18	5.34	6.98	8.06	10.41
Absolute Mean	4.43	4.55	5.46	6.09	8.21
Absolute Standard Deviation	4.45	2.88	4.48	5.44	6.59

visual quality. As a result, this indicates that the adaptive technique can keep more terrain points, thus eliminating vegetation points, than the traditional linear methods.

In general, a visual comparison alone is not sufficient. A better understanding of DTM extraction and their suitability requires testing of their accuracy. Accordingly, it is also of interest to perform a quantitative comparison as a measure of accuracy. As a quality assurance of DTMs, the vertical accuracy of a set of terrain points is first determined by its rms error (RMSE), the square root of the average of the set of squared differences between two points. The RMSE between the "true" values and estimated values is defined as

$$\mathrm{RMSE} = \sqrt{\frac{\sum_{i=1}^{N} (\mathrm{True}_i - \mathrm{estimate}_i)^2}{N}} \tag{12}$$

where N is the number of measurement points, and the "true" sampled data correspond to the surveyed check points. In addition, the height differences between the two DTMs for the surveyed-check points can be analyzed using standard statistical mean and standard deviation to determine the error as well [14]. The mean error and the standard deviation about the error are computed as absolute mean and absolute standard deviation, respectively. The results of the quantitative comparison for all DTMs generated by various techniques are presented in Table I. It is clearly seen that adaptive processing does in fact minimize DTM errors. It is worthy to mention that surveyed data points were provided by Earthdata to justify this statistical analysis.

VI. CONCLUSION

In this paper, an adaptive linear prediction technique for extracting DTMs of the ground surface underlying vegetation is presented. This technique offers, in general, a better tracking capability in the extraction of bare earth models with steep slopes and large variability, which is practically very useful in forestry applications where a true model is not available. Furthermore, it is shown that DTM errors can be minimized through this adaptation process. Note that the iterative process of the adaptive technique requires a selection of the delay, which is done by trial and error in this paper. However, this technique can be significantly improved and fully automated by optimizing both the filter length as well as the delay or prediction order.

ACKNOWLEDGMENT

The authors would like to acknowledge D. Evans and R. King (Department of Forestry and the Department of Electrical and Computer Engineering at Mississippi State University) and N. Eggleston (EarthData) for their contributions to this work as well as the National Aeronautics and Space Administration (NASA) and the Remote Sensing Technology Center (RSTC) at Mississippi State University for their support.

REFERENCES

[1] J. Gong, Z. Li, Q. Zhu, H. Sul, and Y. Zhou, "Effects of various factors on the accuracy of DEMs: An intensive experimental investigation," *ISPRS J. Photogramm. Remote Sens.*, pp. 1113–1117, Sept. 2000.

[2] N. Eggleston, "Tree and terrain measurements from a small-footprint multiple-return airborne LIDAR," Master's thesis, Mississippi State Univ., Mississippi State, 2001.

[3] K. Kraus and N. Pfeifer, "Determination of terrain models in wooded areas with airborne laser scanner data," *ISPRS J. Photogramm. Remote Sens.*, vol. 53, pp. 193–203, 1998.

[4] J. B. Blair and M. A. Hofton, "Modeling laser altimeter return waveforms over complex vegetation using high-resolution elevation-data," *Geophys. Res. Lett.*, vol. 26, no. 16, pp. 2509–2512, 1999.

[5] J. Kilian, N. Haala, and M. Englich, "Capture and evaluation of airborne laser scanner data," *Int. Arch. Photogramm. Remote Sens.*, vol. 31, pp. 383–388, 1996.

[6] N. Pfeifer, T. Reiter, C. Briese, and W. Rieger, "Interpolation of high quality ground models from laser scanner data in forested areas," in *Int. Arch. Photogramm. Remote Sens.*, vol. 32, Nov. 1999, pp. 31–36.

[7] N. Pfeifer, A. Kostli, and K. Kraus, "Interpolation and filtering of laser scanner data – implementation and first results," *Int. Arch. Photogramm. Remote Sens.*, vol. 33, pp. 153–159, 1998.

[8] J. Hyyppa, O. Kelle, M. Lehikonen, and M. Inkinen, "A segmentation-based method to retrieve stem volume estimates from 3-D tree height models produced by laser scanners," *IEEE Trans. Geosci. Remote Sensing*, vol. 39, pp. 969–975, May 2001.

[9] K. Kraus and N. Pfeifer, "A new method for surface reconstruction from laser scanner data," *Int. Arch. Photogramm. Remote Sens.*, vol. 32, pp. 80–86, 1997.

[10] M. Armstrong, *Basic Linear Geostatistics*. Berlin, Germany: Springer-Verlag, 1998.

[11] N. H. Younan, H. S. Lee, D. L. Evans, and N. T. Eggleston, "Extracting digital terrain models in forestry using LIDAR data," *Proc. IGARSS*, July 2001.

[12] M. H. Hayes, *Statistical Digital Signal Processing and Modeling*. New York: Wiley, 1996.

[13] P. M. Clarkson, *Optimal and Adaptive Signal Processing*. Boca Raton, FL: CRC, 1993.

[14] D. F. Maune, *Digital Elevation Model Technologies and Applications: The DEM Users Manual*. Betheda, MD: Amer. Soc. Photogrammetry Remote Sensing, 2001.

Hyun S. Lee (S'99) was born in Korea, in 1970. He received the B.S.E degree in electrical engineering from SungKyunKwan University, Seoul, Korea, in 1996, and the M.S. degree from Mississippi State University, Mississippi State, in 1999. He is currently pursuing the Ph.D. degree at Mississippi State University.

He is currently with Samsung Electronics, Suwon, Korea. His current research interests include applications of signal and image processing, and pattern recognition to remote sensing.

Nicolas H. Younan (S'87–M'88–SM'99) received the B.S.E.E. and M.S.E.E. degrees from Mississippi State University, Mississippi State, in 1982 and 1984, respectively, and the Ph.D. degree in electrical engineering from Ohio University, Athens, in 1988.

He has been with the Department of Electrical and Computer Engineering at Mississippi State University since 1988, where he is currently a Professor. His research interests include the application of advanced signal processing techniques to automated pattern recognition in hyperspectral remote sensing.

Dr. Younan is a Member of Sigma Xi, Tau Beta Pi, Etta Kappa Nu, and Phi Kappa Phi.